Volume 2
Number 7
7 April 2021
Pages 2143–2446

Materials Advances

rsc.li/materials-advances

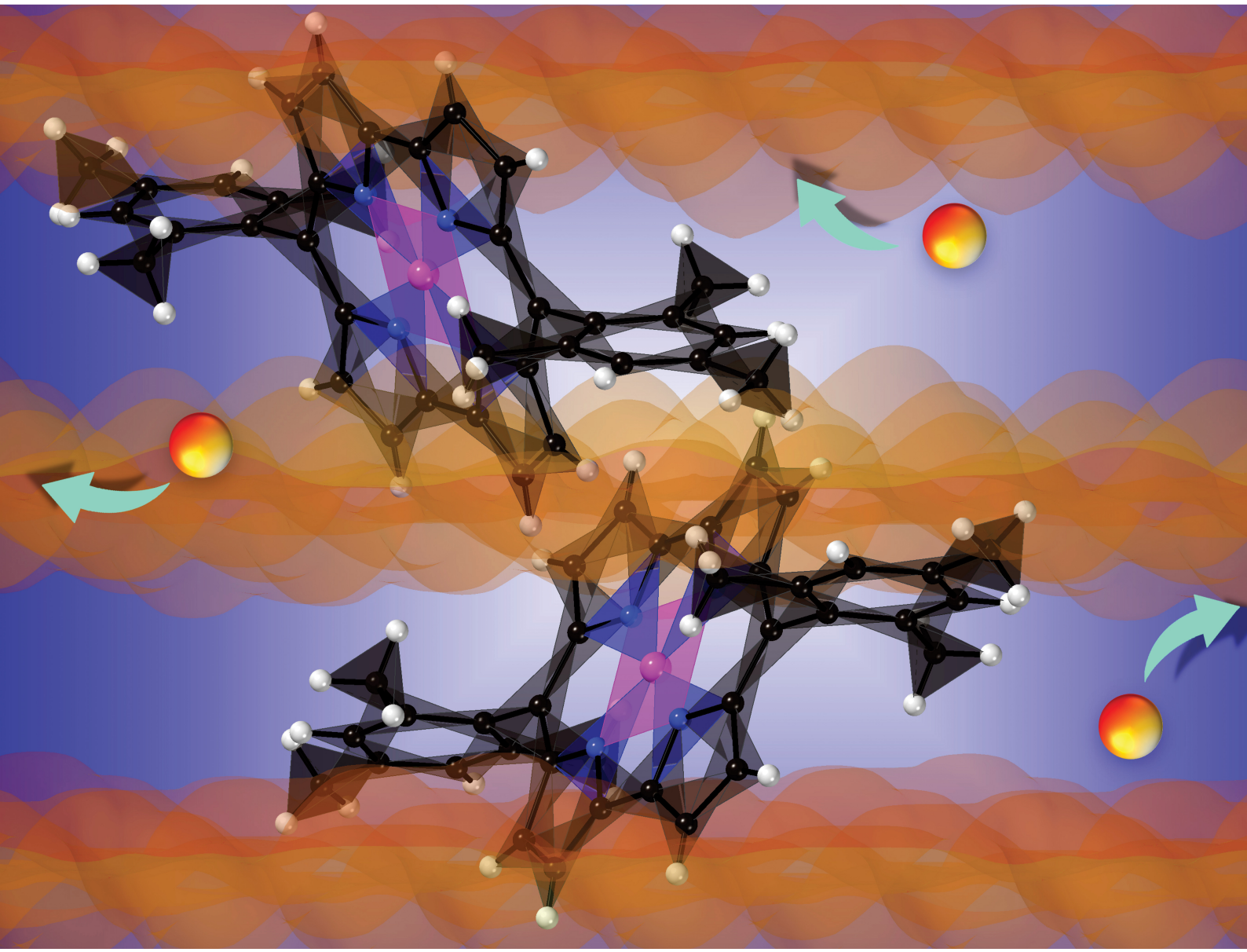

ISSN 2633-5409

ROYAL SOCIETY OF CHEMISTRY

COMMUNICATION

Ji-Young Shin *et al.*

Dual-ion charge–discharge behaviors of Na–NiNc and NiNc–NiNc batteries

Materials Advances

ROYAL SOCIETY OF CHEMISTRY

COMMUNICATION

View Article Online
View Journal | View Issue

Cite this: *Mater. Adv.*, 2021, 2, 2263

Received 5th January 2021,
Accepted 7th March 2021

DOI: 10.1039/d1ma00007a

rsc.li/materials-advances

Dual-ion charge–discharge behaviors of Na–NiNc and NiNc–NiNc batteries†

Jinkwang Hwang, [a] Rika Hagiwara, [a] Hiroshi Shinokubo [b] and Ji-Young Shin *[b]

Dual-ion sodium-organic secondary batteries were produced with anti-aromatic porphyrinoid, NiNc, as an active electrode material, which exhibited inherent charge–discharge behavior with high discharge capacity, high stability, and high Coulombic efficiency at high current density (132.6 mA h g^{-1} discharge capacity and 99.4% efficiency at the 100th cycle with 1 A g^{-1} of current density and 95.3 mA h g^{-1} discharge capacity and 99.3% efficiency at the 100th cycle with 2 A g^{-1} of current density).

Advanced electrochemical energy storage is an important topic of investigation in our world. The urgency of our global situation provides challenges for the invention of eco-friendly systems.[1] Innovative approaches in current research in secondary or rechargeable lithium and lithium-ion-associated organic and inorganic batteries in portable electronic devices have been tried by many different organizations for commercialization.[2] And inexpensive and highly abundant sodium and sodium-ion (sodium being the fourth most abundant element: 2.36% of the Earth's crust) complementary batteries have been investigated to understand the redox durability of organic frameworks for electrode materials.[3] However, achieving transparent dual-ion mobility, fast charge–discharge rate, enhanced discharge capacity, and Coulombic efficiency with diminished electrolyte parasitic reactions has been challenging in order to succeed in achieving superior battery systems, and an enormous number of in-depth studies have investigated these features.[4] Furthermore, investigations of rechargeable batteries without an alkali metal anode have been pursued to achieve freely redox-switchable and accumulating organic batteries that are capable of satisfying safety considerations. So far, no organic battery has been produced that satisfies this goal.

Anti-aromatic compounds are known to possess unsuitable conformations for practical applications due to anti-aromatic destabilization, which easily distorts the compound's planarity. However, an exceedingly active electrode material with anti-aromaticity, nickel norcorrole (NiNc, Fig. 1), has been reported.[5] NiNc showed significantly stable charge–discharge performances in both lithium-cooperating Li–NiNc and lithium-free NiNc–NiNc secondary batteries.[6] The batteries exhibited appropriately high capacities that do not change over long periods, of over 100 cycles. A maximum discharge capacity of about 207 mA h g^{-1} was obtained with Li–NiNc batteries. NiNc has been noted to be a realistically stable anti-aromatic molecule that is suitable for practical application as an active battery material.

Considering this, the possibility of dual-ion conducting materials was investigated with anti-aromatic NiNc as the cathode and inexpensive alkali metal, sodium, as the anode. The charge–discharge durability of Na–NiNc cells was examined with coin cells fabricated with 70 wt% NiNc cathode (NiNc : CB : PVDF = 70 : 25 : 5; CB, carbon black; PVDF, polyvinylidene fluoride), sodium metal anode, and 50 mol% Na[FSA]-[C_2C_1im][FSA] (C_2C_1im, 1-ethyl-3-methylimidazolium; FSA, bis(fluorosulfonyl)amide) ionic liquid electrolyte. Surprisingly, the battery cell exhibited high redox durability and showed precise ion insertion processes, whose behaviors are consistent with the charge–discharge curves of NiNc investigated through a three-electrode cell configuration. Symmetric NiNc batteries were built using different electrolytes. The ionic insertion behavior was understood by means of comparison of the

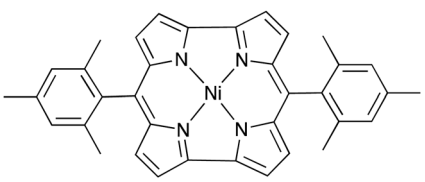

Fig. 1 Structure of *meso*-mesityl nickel norcorrole (NiNc).

[a] *Graduate School of Energy Science, Kyoto University, Kyoto 606-8501, Japan*
[b] *Graduate School of Engineering, Nagoya University, Nagoya 464-8601, Japan. E-mail: jyshin@chembio.nagoya-u.ac.jp; Fax: 81-52-747-6771*

† Electronic supplementary information (ESI) available. See DOI: 10.1039/d1ma00007a

different electrolytes. Herein, we report the first sodium-organic batteries fabricated with an anti-aromatic active electrode. Furthermore, to the best of our knowledge, this is the first non-alkali metal cooperating dual-ion battery with active organic electrodes.

Na–NiNc batteries were prepared using different electrolytes (Fig. S1, ESI†). When 50 mol% Na[FSA]-[C_2C_1im][FSA] electrolyte was applied to the batteries, the charge–discharge performance improved by twice as much as the battery system prepared with 1 M Na[PF_6]-EC/DMC electrolyte (Fig. S2, ESI†). It was considered that the performance improvement was achieved by minimizing the dissolution of high composite NiNc battery electrodes in common organic electrolytes by participating in additional ion pairs (Fig. S3, ESI†). The upper potential of the charging and discharging potential window was optimized to 4.2 V. The 100 cycles of battery performance were monitored in the voltage range of 2.0–4.2 V, with a slow cycling speed (0.2 A g^{-1} of current density), with a plot that successively gave rise to around three electrons involved in the Coulombic efficiency (Fig. S4, ESI†). An optimal cut-off voltage was then fixed in the range of 1.2–4.2 V, where the charge and discharge curves of the Na–NiNc batteries gave sequentially characteristic chemical properties (Fig. 2a). The first redox cycle in the cyclic voltammogram of the Na–NiNc battery was silent until 3.4 V (Fig. 2b and Fig. S5a, ESI†), where Na^+ extraction was appreciably excluded, which can be explained by the three-electrode cell curves in the different charging steps (Fig. 2d and 3a). The durability of the dual-ion charge and discharge performance was evident after the first cycle (Fig. 2e and 3b). Long-term battery performance was then examined to ensure the durability of the discharge capacity and Coulombic efficiency, as shown in Fig. 2c and Fig. S6 (ESI†).

As current density increased, the discharge capacity decreased due to the lack of time to adjust the entirely supplementary polarization (Fig. S7, ESI†). When the current density was set at 1 A g^{-1} for a long-term experiment, as shown in Fig. 2c, 132.6 mA h g^{-1} of discharge capacity and 99.4% efficiency for the 100th cycle were achieved, and these values were retained up to 180 cycles. This performance is in good agreement with involvement of three electrons per molecule. An increased current density, 2 A g^{-1}, resulted in discharge capacities of 95.3, 92.5, 93.1, 91.5, and 90.4 mA h g^{-1} and Coulombic efficiencies of 99.3, 99.6, 99.8, 99.9, and 99.9% for the 100th, 200th, 300th, 400th, and 500th cycles, respectively (Fig. S6, ESI†). The charge–discharge processes offered stabilized performances to give nearly 100% efficiency, which was preserved over 500 cycles. It is a delight that two electrons are involved in the discharge capacities even with the speeded-up charging process.

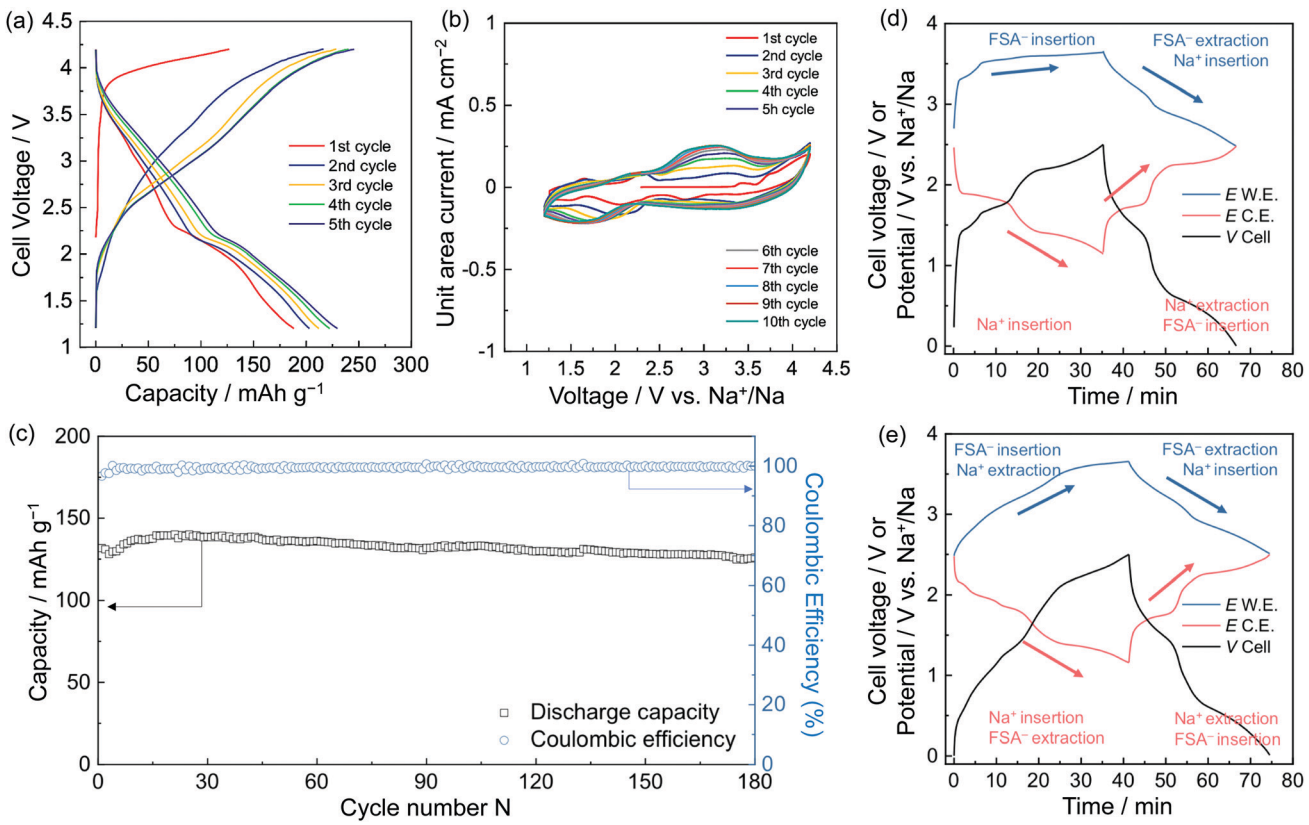

Fig. 2 (a) Selected charge–discharge curves of a Na–NiNc battery consisting of 50 mol% Na[FSA]-[C_2C_1im][FSA] electrolyte: composition of positive electrode = NiNc : CB : PVDF = 70 : 25 : 5 wt%, cut-off voltages = 1.2–4.2 V with a current density of 200 mA g^{-1}. (b) Cyclic voltammogram of the Na–Nc battery. (c) Discharge capacity and Coulombic efficiency plots on a long-period charge–discharge measurement with a Na–NiNc battery consisting of 50 mol% Na[FSA]-[C_2C_1im][FSA] electrolyte (current density = 1 A g^{-1}). (d and e) Dual-ion behavior curves of three-electrode cells for the 1st and the 2nd cycle, respectively.

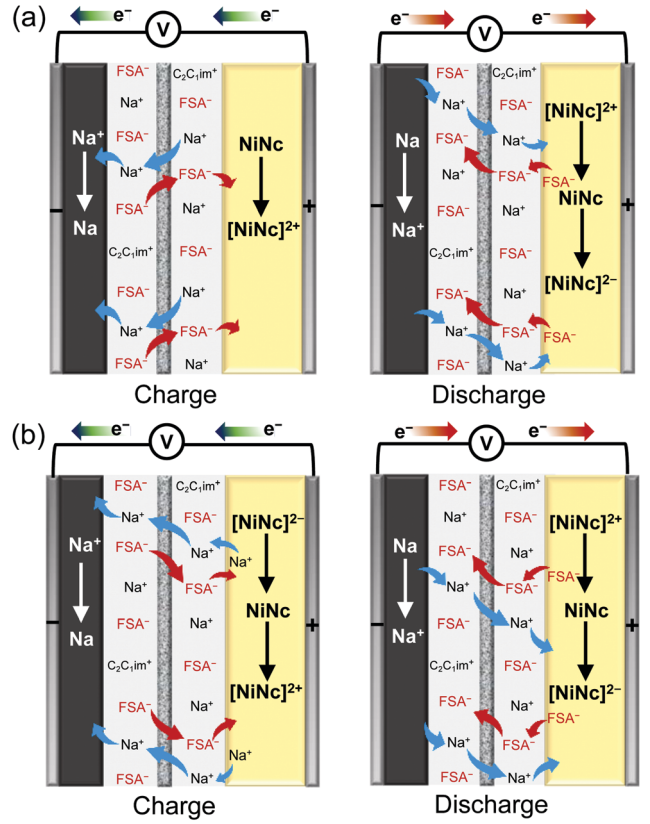

Fig. 3 Schematic perspectives of dual-ion insertion/deletion processes for the first and later cycles: (a) the 1st cycle and (b) the 2nd cycle.

The NiNc electrode behavior was established in the potential ranges 1.2–2.5 V and 2.5–3.7 V *vs.* Na^+/Na for negative and positive electrodes, respectively (Fig. 2d, e and 3). Significantly, the NiNc–NiNc cell processes provided sufficient charge–discharge curves in a range of 0.0–2.5 V, which verified the dual organic electrode conducting networks of the NiNc electrodes (Fig. 4).

The dual organic electrode batteries, NiNc–NiNc batteries, also showed ion-conducting performance (Fig. 4 and Fig. S8, ESI†). The NiNc–NiNc batteries exhibited significantly lower discharge capacities than the Na–NiNc batteries. However, it is notable that those batteries signified dual organic battery behaviors associated with electrolyte ions. The symmetric NiNc–NiNc batteries were assembled with organic solvents of ethylene carbonate (EC)/dimethyl carbonate (DMC), ionic liquids [FSA]-[C_2C_1im][FSA], and 50 mol% Na[FSA]-[C_2C_1im][FSA] electrolytes to refine the influence of dual-ion behavior.

In contrast, the best electrolyte (50 mol% Na[FSA]-[C_2C_1im][FSA]), which afforded excellent charge–discharge performance for Na–NiNc batteries, did not result in the highest capacity for NiNc–NiNc batteries. When Na^+ was removed from the electrolyte, the performance was nearly doubly improved. It was presumed that this was due to the effectiveness of frequent redox switches in the channels of totally symmetric organic electrodes.

The strain of dual-ion insertion/extraction processes confused the mobilities of distinct charged electrolyte ions, resulting in a narrow operating voltage range for actual charge–discharge performance. The systematic insertion/extraction of anions was only established with [C_2C_2im][FSA] for ion flow, and the absence of ions in the ED/DMC electrolyte failed to improve the charge and discharge performance.

Conclusions

Transparent dual-ion mobility, fast charge–discharge rate, enhanced discharge capacity, and high Coulombic efficiency with diminished electrolyte parasitic reactions for Na-organic batteries were successfully achieved using NiNc active electrodes. A high composition of 70% for the NiNc electrodes satisfied inherent charge–discharge behaviors with high discharge capacity, high stability, high Coulombic efficiency and high current densities for charging. Furthermore, symmetric NiNc–NiNc batteries exhibited significantly conserved charge–discharge processes with the dual organic electrodes.

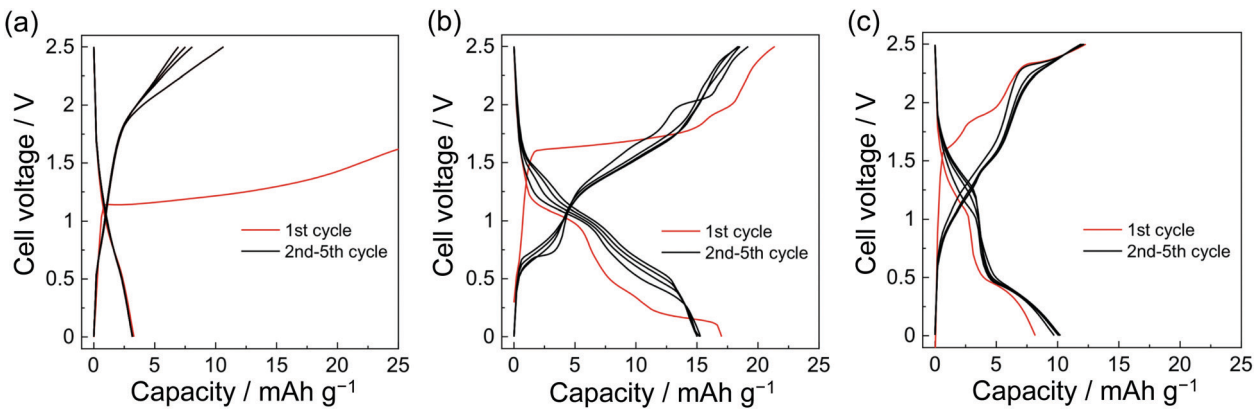

Fig. 4 Charge–discharge performance of symmetric NiNc–NiNc batteries assembled with distinct electrolytes: (a) EC/DMC, (b) [C_2C_1im][FSA], and (c) 50 mol% Na[FSA]-[C_2C_1im][FSA]. Current density and cut-off voltages were set as 50 mA g^{-1} and 0–2.5 V.

Conflicts of interest

There are no conflicts to declare.

Acknowledgements

This research was supported by JSPS KAKENHI Grant Number JP18K04925. J.-Y. Shin acknowledges the Graduate School of Engineering, Nagoya University, for analytical instrumental support. J.-Y. Shin and J. Hwang acknowledge Prof. K. Matsumoto at the Graduate School of Energy Science, Kyoto University, for his appreciated support and advice.

Notes and references

1 M. Armand and J.-M. Tarascon, *Nature*, 2008, **451**, 652.

2 (*a*) A. R. Armstrong and P. G. Bruce, *Nature*, 1996, **381**, 499; (*b*) J. M. Tarascon and M. Armand, *Nature*, 2001, **414**, 356; (*c*) B. Scrosati, *Nat. Nanotechnol.*, 2007, **2**, 598; (*d*) H. Nishida and K. Oyaizu, *Science*, 2008, **319**, 737; (*e*) A. S. Aricó, P. Bruce, B. Scrosati, J.-M. Tarascon and W. V. Schalkwijk, *Nat. Mater.*, 2005, **4**, 368; (*f*) T. Nokami, T. Matsuo, Y. Inatomi, N. Hojo, T. Tsukagoshi, H. Yoshizawa, A. Shimizu, H. Kuramoto, K. Komae, H. Tsuyama and J.-I. Yoshida, *J. Am. Chem. Soc.*, 2012, **134**, 19694; (*g*) Y. Hanyu and I. Honma, *Sci. Rep.*, 2012, **49**, 453; (*h*) Z. Luo, L. Liu, Q. Zhao, F. Li and J. Chen, *Angew. Chem.*, 2017, **129**, 12735 (*Angew. Chem. Int. Ed.*, 2017, **56**, 12561); (*i*) Z. Song, T. Xu, M. L. Gordin, Y.-B. Jiang, L.-T. Bae, Q. Ziao, H. Zhan, J. Liu and D. Wang, *Nano Lett.*, 2012, **12**, 2205; (*j*) X. Li, Z. Hou, W. Huang, H.-S. Xu, X. Wang, W. Yu, R. Li, K. Zhang, L. Wang, Z. Chen, K. Xie and K. P. Loh, *ACS Energy Lett.*, 2020, **5**, 3498.

3 (*a*) J. M. Lee, G. Siingh, W. Cha, S. Kim, J. Yi, S.-J. Hwang and A. Vinu, *ACS Energy Lett.*, 2020, **5**, 1939; (*b*) S. Komaba, W. Murata, T. Ishikawa, N. Yabuuchi, T. Ozeki, T. Nakayama, A. Ogata, K. Gotoh and K. Fujiwara, *Adv. Funct. Mater.*, 2011, **21**, 3859; (*c*) W. Wang, W. Li, S. Wang, Z. Miao, H. K. Liu and S. Chou, *J. Mater. Chem. A*, 2018, **6**, 6183; (*d*) Y. Lee, S. M. Oh, B. Park, B. U. Ye, N.-S. Lee, J. M. Baik, S.-J. Hwang and M. H. Kim, *CrystEngComm*, 2017, **19**, 5028; (*e*) S. M. Oh, I. Y. Kim, S. B. Patil, B. Park, J. M. Lee, K. Adpakpang, S. A. Chae, O. H. Han and S.-J. Hwang, *ACS Appl. Mater. Interfaces*, 2017, **9**, 2249; (*f*) W. Cha, I.-Y. Kim, J. M. Lee, S. Kim, K. Ramadass, K. Gopalakrishnan, S. Premkumar, S. Umapathy and A. Vinu, *ACS Appl. Mater. Interfaces*, 2019, **11**, 27192; (*g*) S. Y. Lim, J. H. Lee, S. Kim, J. Shin, W. Choi, K. Y. Chung, D. S. Jung and J. W. Choi, *ACS Energy Lett.*, 2017, **2**, 998; (*h*) L. Wang, C. Wang, N. Zhang, F. Li, F. Cheng and J. Chen, *ACS Energy Lett.*, 2017, **2**, 256; (*i*) J. Ni, L. Li and J. Lu, *J. Nanosci. Nanotechnol.*, 2010, **10**, 21; (*j*) S. Nandal, M. V. Lee, J. P. Hill, A. Vinu and K. Ariga, *J. Nanosci. Nanotechnol.*, 2010, **10**, 21; (*k*) I. Y. Kim, S. Kim, X. Jin, S. Premkumar, G. Chandra, N.-S. Lee, G. P. Mane, S.-J. Hwang, S. Umapathy and A. Vinu, *Angew. Chem.*, 2018, **130**, 17381 (*Angew. Chem., Int. Ed.*, 2018, **57**, 17137); (*l*) B. Park, S. M. Oh, Y. K. Jo and S.-J. Hwang, *Mater. Lett.*, 2016, **178**, 79; (*m*) B. Park, S. M. Oh and X. Jin, *Chem. – Eur. J.*, 2017, **23**, 6544; (*n*) P. Xiong, R. Ma, N. Sakai, L. Nurdiwijayanto and T. Sasaki, *ACS Energy Lett.*, 2018, **3**, 997; (*o*) Y. Shynkarenko, M. I. Bodnarchuk, C. Benrnasconi, Y. Berezovska, V. Verteletskyi, S. T. Ochsenbein and M. V. Kovalenko, *ACS Energy Lett.*, 2020, **5**, 2835; (*p*) H. Wan, W. Weng, F. Han, L. Cai, C. Wang and X. Yao, *Nano Today*, 2020, **33**, 100860; (*q*) L. Yang, P. Wang, S. Zhang, Y. Wang, L. Zang, H. Zhu, J. Yin and H. Y. Yang, *J. Mater. Chem. A*, 2020, **8**, 22791; (*r*) H. Wan, L. Cai, Y. Yao, W. Weng, Y. Feng, J. P. Mwizerwa, G. Liu, Y. Yu and X. Yao, *Small*, 2020, 2001574; (*s*) M. Sheng, F. Zhang, B. Ji, X. Tong and Y. Tang, *Adv. Energy Mater.*, 2017, **7**, 1601963; (*t*) D. Xie, M. Zhang, L. Xiang and Y. Tang, *Adv. Funct. Mater.*, 2020, **30**, 1906770; (*u*) A. Yu, Q. Pan, M. Zhang, D. Xie and Y. Tang, *Adv. Funct. Mater.*, 2020, **30**, 2001440; (*v*) S. Mu, Q. Liu, P. Kidkhunthod, X. Zhou, W. Wang and Y. Tang, *Natl. Sci. Rev.*, 2020, DOI: 10.1093/nsr/nwaa178.

4 (*a*) H. Sun, Z. Cao, T. Wang, R. Lin, Y. Liu, L. Zhang, F. Lin, Y. Huang and W. Luo, *Mater. Today Energy*, 2019, **13**, 145; (*b*) A. Manthiram, A. V. Murugan, A. Sarkar and T.Muraliganth, *Energy Environ. Sci.*, 2008, **1**, 621; (*c*) Z. Wu, S. Cui, Z. Zhuo, W. Yang, X. Wang and F. Pan, *ACS Appl. Mater. Interfaces*, 2015, **7**, 25105; (*d*) X. Liu, S. Wang, L. Wang, K. Wang, X. Wu, P. Zhou, Z. Miao, Y. Zhao and S. Zhuo, *J. Power Sources*, 2019, **438**, 227017; (*e*) H. H. Sun, H.-H. Ryu, U.-H. Kim, J. A. Weeks, A. Heller, Y.-K. Sun and C. B. Mullins, *ACS Energy Lett.*, 2020, **5**, 1136.

5 T. Ito, Y. Hayashi, S. Shimizu, J.-Y. Shin, N. Kobayashi and H. Shinokubo, *Angew. Chem.*, 2012, **124**, 8670 (*Angew. Chem. Int. Ed.*, 2012, **51**, 8542).

6 J.-Y. Shin, T. Yamada, H. Yoshikawa, K. Awaga and H. Shinokubo, *Angew. Chem.*, 2014, **126**, 3160 (*Angew. Chem. Int. Ed.*, 2014, **53**, 3096).